Effects of Ru doping on the transport and magnetic properties of a $La_{1.32}Sr_{1.68}Mn_{2-y}Ru_yO_7$ layered manganite system

2010 J. Phys.: Condens. Matter 22 236003

(http://iopscience.iop.org/0953-8984/22/23/236003)

IOP Publishing Journal of Physics: Condensed Matter

J. Phys.: Condens. Matter **22** (2010) 236003 (7pp) doi:10.1088/0953-8984/22/23/236003

Effects of Ru doping on the transport and magnetic properties of a $La_{1.32}Sr_{1.68}Mn_{2-y}Ru_yO_7$ layered manganite system

M Kumaresavanji[1], L L L Sousa[2], F L A Machado[2], C Adriano[3], P G Pagliuso[3], E M B Saitovitch[1] and M B Fontes[1]

[1] Centro Brasileiro de Pesquisas Fisicas—CBPF, Rua Dr Xavier Sigaud 150, Urca, Rio de Janeiro, RJ, Brazil

[2] Departamento de Fisica, Universidade Federal de Pernambuco—UFPE, Recife, PE, Brazil

[3] Instituto de Fisica Gleb Wataghin, Universidade Estadual de Campinas—UNICAMP, Campinas, SP, Brazil

E-mail: vanji.hplt@gmail.com

Received 4 March 2010, in final form 13 April 2010
Published 21 May 2010
Online at stacks.iop.org/JPhysCM/22/236003

Abstract

The low temperature magnetization, specific heat, electrical resistance and magnetoresistance have been studied for the Ru-doped $La_{1.32}Sr_{1.68}Mn_{2-y}Ru_yO_7$ ($y = 0.0$, 0.04, 0.08 and 0.15) layered manganite system. The undoped compound ($y = 0.0$) shows a sharp ferromagnetic transition (T_C) accompanied by a metal–insulator transition (T_{MI}) at 118 K. The Ru substitution decreases the T_C and T_{MI} temperatures significantly. The temperature dependence of specific heat measurement confirms the decrease in T_C by observing the anomaly corresponding to T_C. The decreased effective moments from 3.48 μ_B for the undoped compound to 1.82 μ_B for the highly doped compound at 5 K indicates the Ru substitution weakens the ferromagnetic order in the low temperature regime and reduces the number of Mn pairs in the highly doped sample. The field dependence of magnetization measurements exhibits an enhancement of the coercive field with increased Ru concentration and gives evidence for the mixed magnetic phase for the highly doped compound. For the undoped sample, a large negative magnetoresistance of 300% at T_C and 128% at 4.2 K in a 5 T field were observed. The magnetoresistance ratio decreases gradually with increasing Ru substitution. We find that the doped Ru in the Mn site drives the layered manganite system towards a magnetically mixed state. The effects of Ru doping in the transport and magnetic properties will be explained by the antiferromagnetically coupled Ru and Mn sublattices.

1. Introduction

There have been many investigations on perovskite manganese oxides, especially in the $La_{2-2x}A_{1+2x}Mn_2O_7$ layered compound with 'A' a divalent element such as Sr, Ca, Ba and Pb due to their unique features of charge transport and magnetic properties [1–3]. Layered manganites have a rich phase diagram that includes a well-known ferromagnetic (FM) phase that spans a robust range of electronic densities. These behaviors arise out of strongly competing charge, spin and orbital ordering interactions. Theoretical works on doped manganites explained the FM phase and metallicity as caused by the double exchange (DE) interaction [4]. In the DE interaction, the electron hops from Mn^{3+} to O^{2-} which is accompanied by a simultaneous hop from the latter to Mn^{4+}. The probability of this DE electron transfer of an e_g electron depends on the orientation of the neighboring intra-atomic Hund coupled t_{2g} spins. The probability of hopping is also dependent on the Mn–O–Mn bond angle. Such a hopping is a maximum when the magnetic moments of the manganese

ions are aligned parallel and minimum when they are aligned antiparallel. However, metallicity and ferromagnetism are well explained by the DE interaction, it could not adequately explain the paramagnetic insulating phase occurring at high temperature. The presence of a paramagnetic phase is explained by the concept that the mobile electron carries with it the Jahn–Teller distortion of the MnO_6 octahedron [5]. The greater distortion results in more localized charge carriers. This deformation disappears in the metallic state below the ferromagnetic transition.

The parent compound $La_{2-2x}A_{1+2x}Mn_2O_7$ ($x = 0$) is an Mn^{3+}-based antiferromagnetic insulator with no local lattice distortion, and when the amount of divalent element (Ca, Sr, Ba) is increased at the La site it distorts the MnO_6 octahedra. Distortion of the crystal structure changes the inter-atomic distances (Mn–O) and bond angles (Mn–O–Mn), hence influencing the DE interaction. Since the doping of a divalent ion (Sr^{2+} and Ca^{2+}) in the trivalent (La^{3+}) site leads to a mixed valence $La^{3+}_{2-2x}A^{2+}_{1+2x}Mn^{3+}_{2-x}Mn^{4+}_{x}O_7$ system, the doping exhibits peculiar phenomena in charge transport and magnetic properties. Systematic studies on the effects on La site doping by Sr at different doping levels have been widely reported [1, 2, 6]. The increased doping level results in a variety of electrical and magnetic regions, depending on temperature.

The magnetic phase diagram of the $La_{2-2x}Sr_{1+2x}Mn_2O_7$ system, determined by neutron diffraction for a wide range of doping, was reported by Mitchell *et al* [3]. The phase diagram deals with the different resistive and magnetic phases depending on the doping level and temperature. According to the phase diagram, the charge transport and magnetic properties of layered manganites are extremely sensitive to small changes in La site doping and temperature. This system shows a ferromagnetic metal in a narrow doping range $0.30 \leqslant x \leqslant 0.42$. The increased Sr concentration in the La site results in a canted antiferromagnetic order at $0.42 \leqslant x \leqslant 0.5$ and a charge ordered insulator in the half-doped region ($x \simeq 0.5$).

Although the 'A' site doping is an indirect method to achieve ferromagnetism and metallicity by forcing a Mn to change from 3+ ionic valence to 4+, it is interesting to study the Mn site doping, which is rather a direct method. Also, the Mn site doping plays an important role in the carrier density (n), Mn–O bond length and Mn–O–Mn bond angle in controlling the physical properties of these manganites. The Mn site doping not only introduces lattice distortions but also reduces the number of Mn^{3+}/Mn^{4+} pairs. It was found that the metal to insulator transition can be produced by partly replacing Mn with ions such as Fe, Co, Cu, Cr, Ru, Hf and Al, which shift the magnetic and metal–insulator transitions continuously to lower temperature [7–9]. In this paper, the magnetization, specific heat, charge transport and magnetoresistance in the bulk samples of $La_{1.32}Sr_{1.68}Mn_{2-y}Ru_yO_7$ ($y = 0.0$, 0.04, 0.08 and 0.15) have been studied very carefully in order to gain a deeper understanding of the mechanism of DE and the formation of Jahn–Teller polarons by the Ru doping in the Mn sites.

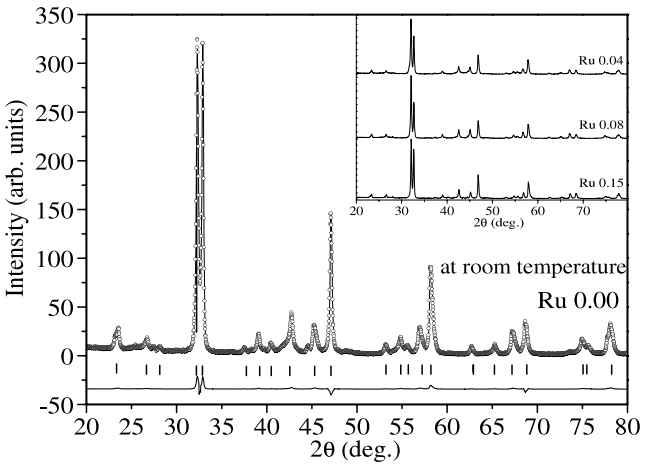

Figure 1. Powder x-ray diffraction pattern recorded at room temperature and processed by the Rietveld method for the $La_{1.32}Sr_{1.68}Mn_2O_7$ system. The inset shows the XRD patterns of Ru-doped samples.

2. Experimental methods

The stoichiometric polycrystalline $La_{1.32}Sr_{1.68}Mn_{2-y}Ru_yO_7$ ($y = 0.0$, 0.04, 0.08 and 0.15) samples were synthesized by the conventional solid-state reaction procedure, as reported in [10]. Care was taken to ensure the preparation is identical for all the samples. The room temperature powder XRD patterns with a step of 0.02° in the 2θ range 20°–80° were recorded with Cu Kα radiation using a Philips diffractometer. The XRD patterns were analyzed with the Rietveld method using the GSAS program and the refined patterns confirmed these samples to be single phase. A commercial SQUID magnetometer (Quantum Design) was used to carry out all the magnetization measurements reported here. The electrical resistance measurements at low temperatures have been performed with the standard four-probe method using the same procedure described in [10]. The low temperature specific heat c_p was measured using a PPMS (Quantum Design) system in the temperature range of 2–300 K. In this system, c_p is determined using a thermal relaxation technique [11]. A very small amount of Apiezon N-grease was used to attach the sample to the calorimeter. Moreover, great care was exercised to subtract the attachments (calorimeter plus N-grease) from the total heat capacity.

3. Results

3.1. X-ray diffraction patterns

Figure 1 shows the powder x-ray diffraction patterns of the $La_{1.32}Sr_{1.68}Mn_{2-y}Ru_yO_7$ ($y = 0.0$, 0.04, 0.08 and 0.15) system recorded at room temperature for all the compounds. The Rietveld refinements agree well with the calculated patterns and the compounds were found to be monophasic. All the diffraction peaks were indexed to the $Sr_3Ti_2O_7$-type tetragonal structure and all the samples belong to the space group $I4/mmm$. The calculated unit cell parameters for the undoped sample, $a = 3.8661$ Å and $c = 20.1759$ Å, are

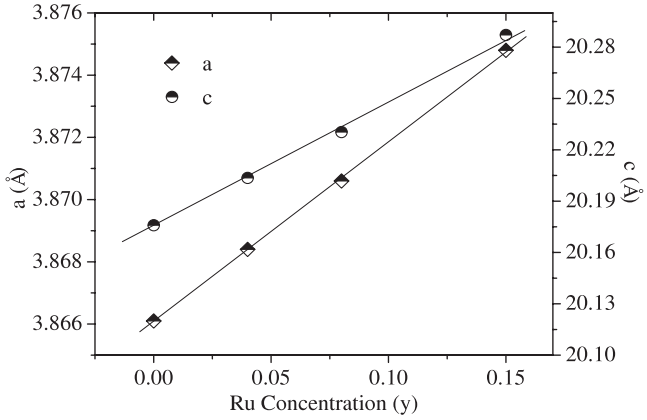

Figure 2. Variation of lattice parameters with the Ru concentration.

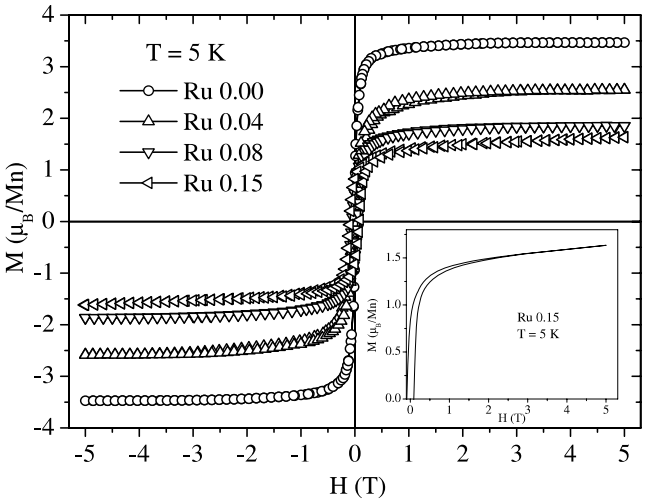

Figure 3. Hysteresis curves measured at 5 K for all the compounds. For better visualization, we show the $M(H)$ curve for the Ru 0.15 compound in the inset.

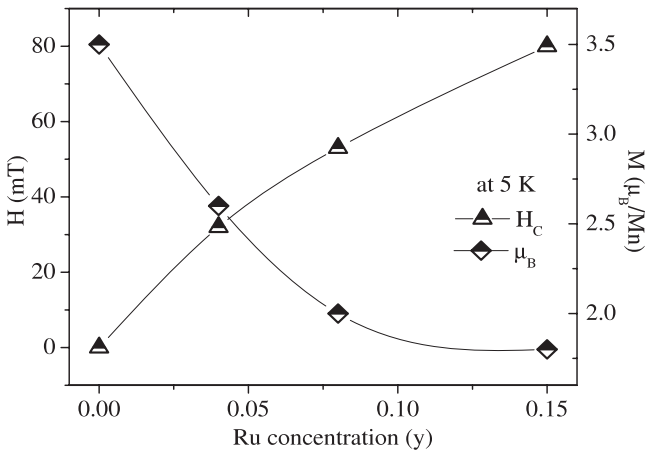

Figure 4. Observed magnetic moments and coercive field dependence of Ru concentration at 5 K.

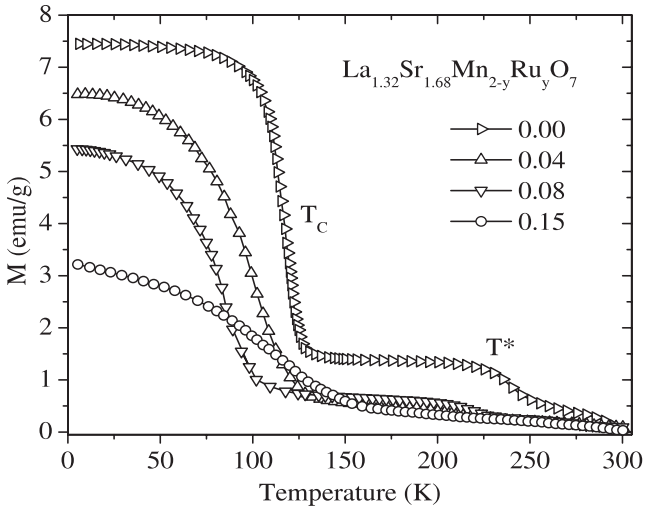

Figure 5. The magnetic moments plotted as a function of temperature for the series $La_{1.32}Sr_{1.68}Mn_{2-y}Ru_yO_7$.

in good agreement with the values reported earlier [12]. The variation of lattice parameters a and c with Ru substitution is shown in figure 2. As is seen in the figure, the lattice parameters are seen to increase linearly as a function of Ru substitution.

3.2. Magnetization measurements

The field dependence of magnetization $M(H)$ measurements were performed for all the samples at 5 K and the results were plotted in figure 3. The samples exhibit a ferromagnetic phase except for the highly doped sample ($y = 0.15$). The highly doped sample does not show any saturation even up to 5 T field, which is shown in the inset of figure 3. We find that the calculated magnetic moments were reduced from 3.48 μ_B for the undoped compound to 1.82 μ_B for the highly doped compound. The reduced magnetic moments are evidence of the influence of Ru pairs in Ru-doped samples. Also, the coercive field is increased to 81 mT for the $y = 0.15$ sample, with increased amount of Ru. The change in magnetic moments and coercive field observed by Ru substitution at 5 K is plotted in figure 4. The $M(H)$ measurements were also performed at room temperature for all the compounds, which is not shown here. The magnetization curves confirm the paramagnetic phase for all the compounds at room temperature.

In figure 5, we show the temperature dependence of magnetization curves (field-cooled (FC) with 100 Oe), which result in a sharp ferromagnetic transition (T_C) at 118 K for the undoped sample. Even above the T_C, we have observed another transition at T^*, which was reported earlier [13, 14]. There is a 2D short range ferromagnetic order between the T_C and T^* temperatures. The 2D ferromagnetic order above T_C is an intrinsic behavior of bilayer manganites. Osborn *et al* [15] also found the two-dimensional short range FM order within the plane above T_C and pointed out the coexistence of the FM and antiferromagnetic (AF) correlation between each plane in the bilayer unit in the $La_{1.2}Sr_{1.8}Mn_2O_7$ compound. Thus, the existence of 2D short range FM order in a wide temperature region above T_C may be related to the anisotropic exchange energy in the quasi-two-dimensional FM system. Increased Ru substitution shifts the T_C to lower temperature values and

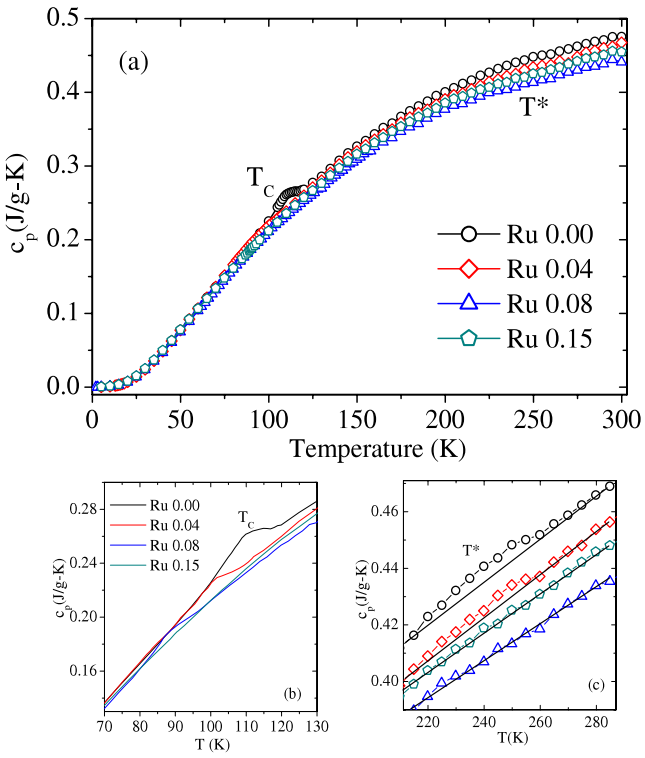

Figure 6. Temperature dependence of specific heat measured in the absence of an applied magnetic field (a). Highlights of the anomalies seen in c_p near T_C and T^* are shown in (b) and (c), respectively. The solid lines in (c) are guides to the eyes.

(This figure is in colour only in the electronic version)

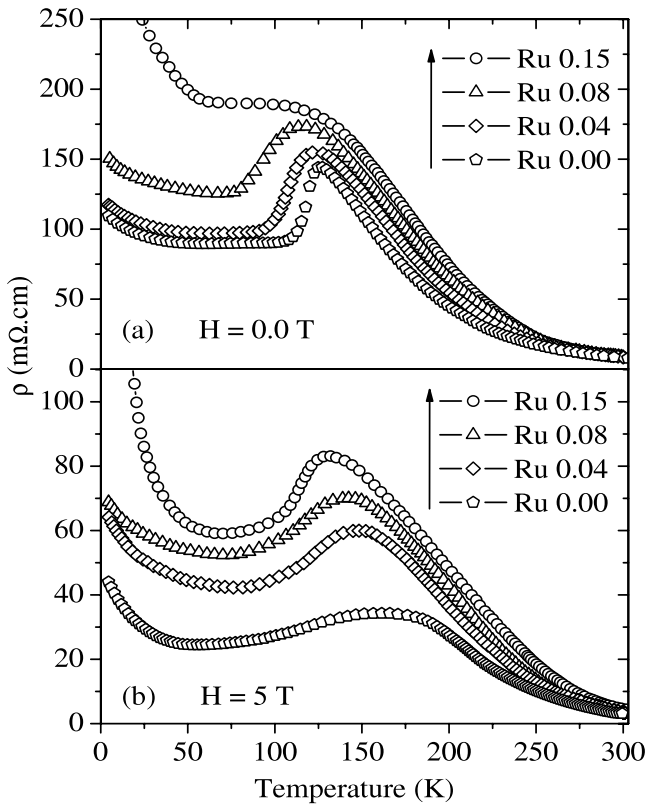

Figure 7. The electrical resistivity plotted as a function of temperature in (a) zero field and (b) at 5 T.

suppresses the T^* temperature in the highly doped sample. All the samples show a ferromagnetic to paramagnetic transition except for the highly doped sample. The highly doped sample shows a mixed state of magnetic orders at low temperature.

3.3. Specific heat measurement

We have measured the temperature dependence of specific heat (c_p) in the absence of an applied magnetic field for all the samples and the results were plotted in figure 6. In this figure, one can see small anomalies in c_p with maxima in the temperature range 80–120 K that are being associated with T_C. The anomaly in the undoped sample is bigger than the one observed for the doped samples (figure 6(b)). The increase in Ru doping shifts the anomalies to lower temperature values continuously at the same rate observed in the $M(T)$ curves. These results are in very good agreement with the magnetization (figure 5) and electrical resistivity (figure 7) data.

Moreover, some even smaller anomalies are observed in c_p near 250 K, which is a temperature close to T^*. The excess near T^* is better seen in figure 6(c). This figure is a blow-up of the high temperature part of the data. Straight lines were drawn to highlight the bumps near T^* for the undoped and for the Ru 0.04 samples and to better indicate the strong suppression of the bumps for higher contents of Ru. These observations are also closely related to the magnetization data presented in figure 5. Unfortunately, the anomalies near T_C and T^* are too small and it is not so easy to estimate the lattice heat capacity which would allow us, for instance, to calculate the entropy associated with the phase transitions and to make a more quantitative analysis. Finally, at lower temperatures the specific heat data show an upturn due to Schottky-type anomalies arising from the interaction of rare earth ions with the crystalline field.

3.4. Electrical resistance and magnetoresistance measurements

In figure 7, we show the temperature dependence of resistivity curves $\rho(T)$ in the absence of external field and at 5 T. The measurements exhibit a sharp T_{MI} transition at 118 K for the undoped sample, which coincides with T_C. The coexistence of the ferromagnetic and metal to insulator transitions is an alternative behavior of magnetic manganites. However, we could not observe any transition related to T^* temperature in the $\rho(T)$ curves. The increased Ru doping decreases the transition temperature gradually and increases the resistivity values abruptly (figure 7(a)). For the highly doped sample we could not observe any metal to insulator transition whereas the sample exhibits an insulating behavior in the whole temperature range. However, the applied 5 T field shifts the T_{MI} to higher temperature values and the field induces a metallic regime in the highly doped sample (figure 7(b)). In order to attribute the high temperature behavior to Jahn–Teller polarons, we have fitted the high temperature regime of

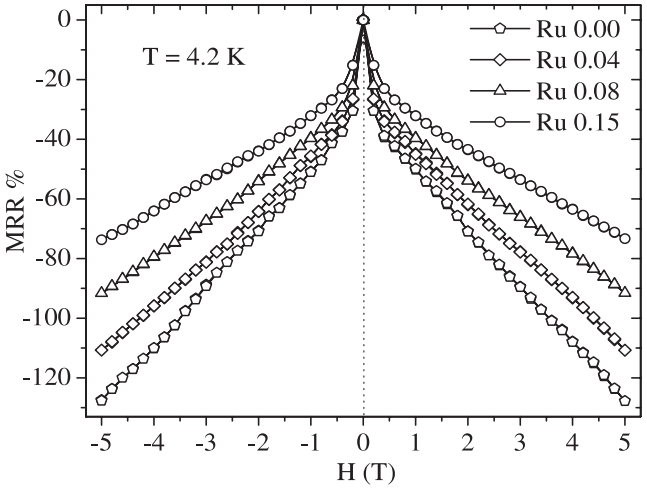

Figure 8. Field dependence of resistivity measured at 4.2 K.

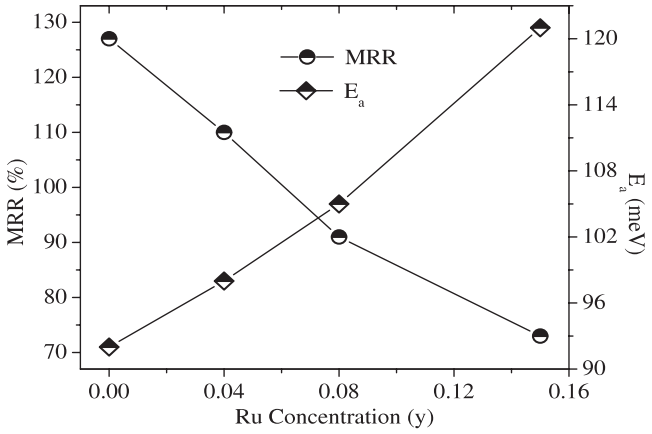

Figure 9. The variation of the magnetoresistance ratio observed at 4.2 K (left-hand scale) and activation energy (right-hand scale) depends on Ru concentration.

$\rho(T)$ curves for Emin–Holstein's polaron hopping model with $\rho = \rho_0 \times \exp[E_a/k_B T]$. The ρ_0, E_a and k_B in the expression denote residual resistance, activation energy and Boltzmann's constant, respectively. The E_a values calculated from the model were plotted in figure 9. As is seen in the figure, the increased Ru substitution in Mn sites increases the activation energy systematically.

The field dependence of resistivity $\rho(H)$ at 4.2 K was measured for all the samples and plotted in figure 8. In the measurement, we have observed a large negative magnetoresistance on the application of an external field of 5 T. The magnetoresistance ratio (MRR) was calculated from the equation MRR $= \frac{\rho_0 - \rho_H}{\rho_H} \times 100$. We have observed a decrease in MRR from 128% for the undoped sample to 72% for the highly doped sample. Figure 9 shows the variation of MRR measured at 4.2 K and the activation energy depending on Ru substitution in the left- and right-hand scale, respectively. For the undoped sample, 300% of MRR was calculated at T_C in a 5 T field from the $\rho(T)$ measurements (figure 7). The MRR was decreased to 80% by increasing Ru substitution.

4. Discussion

The Mn site doping is a direct method to induce a mixed Mn valence between Mn^{3+} and Mn^{4+}, which plays an important role in the charge transport and magnetic properties of perovskite manganites. Many groups studied Mn site doping, replacing Mn by Ge, Sn, Cu, Fe, Zr, Ru, Hf and Al [7–9]. All the studies were carried out in the low doped region. The ground state of $La_{2-2x}Sr_{1+2x}Mn_2O_7$ takes consecutively the ferromagnetic state with $d_{3x^2-r^2}/d_{3y^2-r^2}$ orbital ordering for the doping concentration $0.01 \leqslant x \leqslant 0.23$ and the ferromagnetic state with $d_{x^2-y^2}$ orbital ordering for $0.23 \leqslant x \leqslant 0.34$ [16]. In this paper, we have reported the Ru doping in the $La_{1.32}Sr_{1.68}Mn_2O_7$ system. Several previous studies reported that $La_{1.32}Sr_{1.68}Mn_2O_7$ undergoes a ferromagnetic to paramagnetic transition at 118 K [3, 10, 17]. At temperatures below ~118 K, the magnetic moments on the Mn sites are ferromagnetically coupled both between and within the bilayers.

The appreciable increase in lattice parameters is expected, because the ionic radius of Ru (0.68 Å) is larger than that of manganese (0.52 Å). Hence, the observed increase of lattice parameters confirms the Ru should have a mixed valence of Ru^{4+} and Ru^{5+} with $\langle r \rangle_w = 0.66$ Å [18]. The ferromagnetic saturation value of 3.48 μ_B, observed in the undoped sample, virtually coincides with the values expected from the spin contribution arising from Mn^{3+} and Mn^{4+} ions. Since, in the low spin state, the values of μ_B are 2.83 and 1.73 μ_B for Ru^{4+} and Ru^{5+}, respectively [19], the values of magnetic moments between 3.48 and 1.82 μ_B in our study confirm the mixed states of Ru should be in between Ru^{4+} and Ru^{5+}. The presence of Ru^{4+} and Ru^{5+} are also confirmed by the XPS spectroscopic study of the $La_{1-x}Sr_xMn_{1-y}Ru_yO_3$ system [20]. So it is proposed that in our study there is an interplay of mixed Zener pairs such as Mn^{3+}/Mn^{4+}–Ru^{4+}/Ru^{5+}. The relative fraction of Ru mixed valence (Ru^{4+} and Ru^{5+}) is regulated by the Ru concentration (y).

The increased amount of Ru in the Mn site affects the transport behavior significantly, especially at low temperature, shifting the transition temperatures (T_C and T_{MI}) towards lower temperature values and enhancing the coercive field. For the undoped sample, we could not observe any coercive field. In the highly doped sample, the Ru doping increases the coercive field to 81 mT. In the measurement, it is revealed that the Ru content makes the system magnetically hard. However, the magnetic moments at low temperature decrease from 3.48 μ_B to 1.82 μ_B by increasing the Ru substitution. The decreased magnetic moments with increased Ru doping is evidence for the domination of Ru pairs and dilution of Mn pairs. The decrease of T_C is also evidence for the suppression of 3D ferromagnetic order by Ru content. However, the highly doped sample shows a mixed magnetic state. The $M(H)$ and $M(T)$ measurements confirm the existence of a mixed state of ferromagnetic and antiferromagnetic orders in the highly doped sample.

The specific heat measurement gives evidence for the existence of T_C and T^* temperatures (figure 6). The

temperature dependence of resistivity and magnetization measurements show that a metal–insulator transition (T_{MI}) coincides with the ferromagnetic to paramagnetic transition (T_C). The coexistence of T_C and T_{MI} is an intrinsic feature of perovskite manganites [21]. The low temperature ferromagnetic metal is explained by the DE interaction, whereas the high temperature paramagnetic insulator is explained by the formation of Jahn–Teller polarons. The upturn observed below 30 K in the $\rho(T)$ curves is due to the localization effect, perhaps a two-dimensional confinement of e_g carriers at low temperature. With increased Ru content the upturn enhances and the highly doped sample shows an insulating behavior in the whole temperature range. The calculated activation energy values increase with increased Ru doping, indicating that the addition of Ru enhances the formation of Jahn–Teller polarons. The trapping of charge carriers is more effective due to greater distortion of the MnO_6 octahedron. So, we argue that there is a strong Jahn–Teller distortion on substitution of Ru.

Since the exchange interaction and Jahn–Teller polaron formation occurring in manganite compounds are determined by the interactions within the Mn–O–Mn network, any substitution into this network drastically modifies the physical properties. Due to the itinerant Ru 4d electrons and extended 4d orbitals, strong hybridization between Ru 4d and O 2p is present. Therefore, oxygen-mediated Mn–Ru magnetic coupling is expected to be stronger than Mn–Mn coupling and has an opposite sign. It is obvious that the Mn^{3+}/Mn^{4+} pair is an essential ingredient for the DE interaction, which makes the system ferromagnetically metallic. When Ru is substituted instead of Mn, the Ru low spin pairs Ru^{4+}/Ru^{5+} dominate in the doped sample and weaken the DE interaction. The decrease of T_{MI}, as well as the increase of resistivity with increasing Ru content, shows that the interaction between Mn and Ru is superexchange rather than DE.

The antiferromagnetic order occurring in the highly doped sample can be explained by the antiferromagnetically coupled Ru and Mn pairs. We assume an antiparallel coupling of Ru (Ru^{4+} and Ru^{5+}) and Mn (Mn^{3+} and Mn^{4+}) magnetic moments. For low doped concentration Mn moments are aligned parallel and Ru ions are aligned antiparallel by interaction with all the neighboring Mn ions. In the high doping level, the Ru moments increase and therefore the total moments of the whole system could be antiferromagnetically coupled. Our experimental results, where the highly doped sample shows an antiferromagnetic insulating phase, also confirm the above assumption. Weigand *et al* studied the x-ray magnetic circular dichroism for the Ru-doped $La_{1.2}Sr_{1.8}Mn_{2-x}Ru_xO_7$ system and found an unexpected antiferromagnetic sublattice coupling between manganese and ruthenium [22]. Taking account of the above discussion, we argue from our $M(T)$ and $\rho(T)$ measurements that the Ru substitution drives the system to an antiferromagnetic insulator because of the antiferromagnetically coupled Ru and Mn magnetic moments.

According to Zener [4], the DE is possible only for the ferromagnetically coupled spin states. Since, in our case, the low spin Ru is antiferromagnetically coupled with Mn, the conduction process is expected by the superexchange interaction. Hence, we argue that the substitution of Ru induces a phase separation with the existence of ferromagnetically coupled DE and antiferromagnetically coupled superexchange interactions in the low temperature regime. The increased activation energy and resistivity values with increased Ru substitution is also evidence for the weakening of ferromagnetic order and DE interaction. However, the applied field induces a metal–insulator transition in the highly doped sample (figure 7(b)). Since the antiparallely coupled Ru is aligned with the external field, the Mn and Ru will be coupled ferromagnetically. Hence, a metal–insulator transition can be obtained by an external field.

The MR is simply related to the reduction of spin fluctuations by an applied magnetic field [23]. Indeed, the MR observed in the layered manganite system is explained in terms of inter-bilayer tunneling magnetoresistance (TMR), because of the ferromagnetic metallic MnO_2 bilayers which are separated by a nonmagnetic $(La, Sr)_2O_2$ insulating layer stacked along the c axis [24]. Thus the bilayer manganite can be viewed as an infinite array of ferromagnetic metal (FMM)–insulator (I)–FMM junctions or an infinite stack of spin valves. In polycrystalline samples, the MR is dominated by the spin-polarized tunneling and the tunneling process takes place across the interfaces or grains separated by the insulating barrier. The MRR observed in the layered system is much higher than observed in cubic perovskite manganites because of the high spin polarization of conduction electrons. According to the tunneling model, the change in tunneling resistance is closely related to the spin polarization of conduction electrons in each FM layer [25, 26]. The ferromagnetically coupled intralayers lead to a greater tunneling of electrons, whereas the antiferromagnetic coupled layers lead to a lower tunneling. In our measurements, a large negative MR of about 300% at T_C and 128% at 4.2 K was observed for the undoped sample. The Ru substitution gradually reduces MRR to lower values, in particular at T_C. Since the Ru and Mn are antiferromagnetically coupled, the tunneling process does not take place effectively. As a result, the MRR is reduced with increasing Ru concentration.

5. Conclusion

In conclusion, the charge transport and magnetic properties of the $La_{1.32}Sr_{1.68}Mn_{2-y}Ru_yO_7$ system have been investigated by low temperature magnetization, specific heat, electrical resistance and magnetoresistance, and we find that the Ru substitution affects these properties significantly. The transition temperature is seen to decrease as a function of Ru doping and an antiferromagnetic insulating behavior has been observed for the highly doped sample. These results were inferred by the antiferromagnetically coupled Ru 4d and Mn 3d orbitals, which play an important role in the exchange interaction. The charge transport occurring in Ru-doped samples is attributed to the superexchange interaction. The decreased magnetic moments and increased activation energy by Ru substitution also confirmed the dilution of ferromagnetic order and DE interactions. Hence,

our results suggest that the Ru induces a phase separation scenario with the presence of ferromagnetically coupled DE and antiferromagnetically coupled superexchange interactions in the low temperature regime. A spin-polarized inter-grain tunneling magnetoresistance has been observed at low temperature in the external field of 5 T. Ru substitution reduces the MRR significantly due to the antiferromagnetically coupled Ru in the Mn site. Hence, we claim that the Ru is found to be an effective tool to modify the Mn–O–Mn network and participate in the charge transport and magnetic properties of the layered manganite.

Acknowledgments

MK acknowledges the Conselho Nacional de Desenvolvimento Cientifico e Tecnologico (CNPq), Brazil and the Third World Academy of Sciences (TWAS), Italy for the award of a CNPq-TWAS fellowship. This work is supported by the funding agencies Edital Universal-CNPq grant no. 470940/2007-7, APQ1-FAPERJ grant no. E26/170.717/2007, Pronex-FAPERJ grant no. E-26/171.165/2003 and Cientistas do Estado-FAPERJ grant no. E-26/102.700/2008.

References

[1] Kimura T and Tokura Y 2000 *Annu. Rev. Mater. Sci.* **30** 451
[2] Ling C D, Millburn J E, Mitchell J F, Argyriou D N, Linton J and Bordallo H N 2000 *Phys. Rev.* B **62** 15096
[3] Mitchell J F, Ling C D, Millburn J E, Argyriou D N, Berger A and Medarde M 2001 *J. Appl. Phys.* **89** 6618
[4] Zener C 1951 *Phys. Rev.* **82** 403
[5] Millis A J, Littlewood P B and Shraiman B I 1995 *Phys. Rev. Lett.* **74** 5144
[6] Wang A and Cao G 2006 *J. Magn. Magn. Mater.* **305** 520
[7] Zhang J, Yan Q, Wang F, Yuan P and Zhang P 2000 *J. Phys.: Condens. Matter* **12** 1981
[8] Sahu R K, Sundar Manoharan S, Mohammad Q, Rao M L and Nigam A K 2002 *J. Appl. Phys.* **91** 7724
[9] Nair S and Banerjee A 2004 *Phys. Rev.* B **70** 104428
[10] Kumaresavanji M, Reis M S, Xing Y T and Fontes M B 2009 *J. Appl. Phys.* **106** 093709
[11] Machado F L A and Clark W G 1988 *Rev. Sci. Instrum.* **59** 1176
[12] Kubota M, Fujioka H, Hirota K, Ohoyama K, Moritomo Y, Yoshizawa H and Endoh Y 2000 *J. Phys. Soc. Japan* **69** 1606
[13] Wang A, Cao G, Liu Y, Long Y, Li Y, Feng Z and Ross J H 2005 *J. Appl. Phys.* **97** 103906
[14] Argyriou D N, Mitchell J F, Potter C D, Bader S D, Kleb R and Jorgensen J D 1997 *Phys. Rev.* B **55** R11965
[15] Osborn R, Rosenkranz S, Argyriou D N, Doloc L V, Lynn J W, Sinha S K, Mitchell J F, Gray K E and Bader S D 1998 *Phys. Rev. Lett.* **81** 3964
[16] Zhang Q, Zhang W and Jiang Z 2005 *Phys. Rev.* B **72** 142401
[17] Okuda T, Kimura T and Tokura Y 1999 *Phys. Rev.* B **60** 3370
[18] Shannon R D and Prewitt C T 1969 *Acta Crystallogr.* B **25** 925
[19] Butera A, Fainstein A, Winkler E and Tallon J 2001 *Phys. Rev.* B **63** 054442
[20] Ying Y, Fan J, Pi L, Qu Z, Wang W, Hong B, Tan S and Zhang Y 2006 *Phys. Rev.* B **74** 144433
[21] Dagotto E, Hotta T and Moreo A 2001 *Phys. Rep.* **344** 1
[22] Weigand F, Gold S, Schmid A, Geissler J, Goering E, Dorr K, Krabbes G and Ruck K 2002 *Appl. Phys. Lett.* **81** 2035
[23] Siwach P K, Singh H K and Srivastava O N 2008 *J. Phys.: Condens. Matter* **20** 273201
[24] Kimura T, Tomioka Y, Kuwahara H, Asamitsu A, Tamura M and Tokura Y 1996 *Science* **274** 1698
[25] Julliere M 1975 *Phys. Lett.* A **54** 225
[26] Moodera J S, Nassar J and Mathon G 1999 *Annu. Rev. Mater. Sci.* **29** 381